High-temperature Superconducting Interconnects for Ultra-low Temperature, High-field Environments

Vyacheslav Solovyov, Hyunwoo Kim, and Paul Farrell

***Abstract*— Coplanar (with the ground) 20 cm long waveguides are manufactured from the YBCO-on-Kapton material. We investigate the effect of parasitic ground plane resonances on the performance of these waveguides. It is concluded that dense rows stitching vias are essential for isolating the lines to a level below 60 dB at 6 GHz. We demonstrate a metalized via technology that is compatible with both the traditional Flexible Printed Circuit (FPC) process and the epitaxial YBCO material. Stitching via fence with the via period 10 mm is shown as effective in suppressing parasitic resonances at 77 K.**

***Index Terms*— High-temperature superconductors, quantum computing, RF properties, parasitic resonances.**

I. Introduction

THE efficient delivery of electric signals and power from a room temperature environment to a cryogenic device is a well-recognized challenge. Both resistive and conduction losses account for a significant portion of a cryo-cooling system load. In normal metals, electrons are carriers of both charge and thermal energy, which results in a constant ratio between thermal and electric conductivity, the effect known as the Wiedemann-Franz (WF) law.

Cryogenic RF signal cables are also subjected to the limitation of the WF law because the RF loss is proportional to the bulk electric resistivity of the cable material. Fig. 1 illustrates this point by presenting the relationship between RF attenuation, α_t, and linear thermal conductance (per unit length of the cable), κ, for commercial cryogenic RF cable products offered by the major manufacturers. The solid line is an empirical best-fit approximation of the $\kappa \sim \alpha_t^{-1.5}$. Clearly, low RF attenuation is achieved at the expense of high thermal conductance. The horizontal line indicates the maximum allowable thermal conductivity of an RF line in a hypothetical device with 1,000 lines cooled by a Bluefors XLD cooler equipped with a 1.5 W PT415 Cryomech pulsed tube cryocooler. The graph shows that in such a device, only a few regular metal cable products, such as an ultra-thin, 0.33 mm diameter SC-033 SS cable by Coax LTD would not overload the cryocooler by the passive thermal conduction losses.

In superconductors, the WF law is violated by the formation of a coherent ground state. Several Nb and NbTi coaxial RF cables have demonstrated a combination of low insertion loss and low thermal conductivity [1-3]. For a loss-constrained cryogenic application, a thin film line is preferred because it is straight forward to implement controlled impedance and maximize the cross-sectional area over which the RF current flows. Indeed, cables manufactured from thin Nb films deposited on Kapton have shown promise as interconnects for large quantum computing systems [4].

The Nb-based devices can function well below the critical temperature of the material, 9.2 K for Nb and 9.7 K for NbTi. High-energy physics detectors often operate in a magnetic field exceeding the upper critical field of NbTi, ≈ 8 T at 4 K. An example of a quantum detection system is the Axion Dark Matter eXperiment [5], which searches for dark-matter axions using an axion haloscope. The haloscope consists of a microwave-resonant cavity inside a strong, up to 10 Tesla, magnetic field. The experiment sensitivity can be significantly improved by the implementation of a superconducting RF readout cable capable of operating in 10 Tesla field, < 4 K.

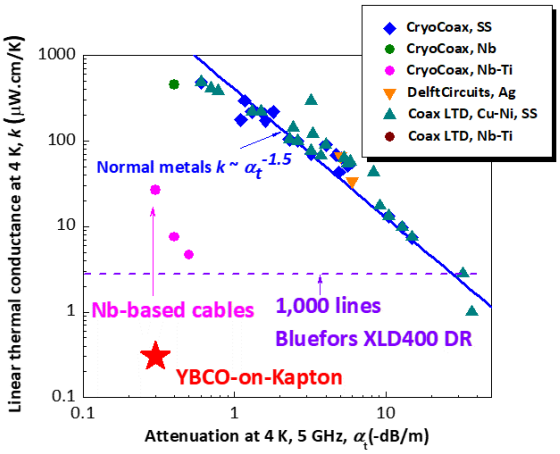

Fig. 1. Linear thermal conductance (per unit length of the cable) κ at 4 K vs. attenuation α_t (5 GHz, 4 K) for commercial cryogenic RF cables. The solid line is an empirical best-fit approximation of the $\kappa \sim \alpha_t^{-1.5}$ for cables manufactured from normal (non-superconducting) metals. The filled circles indicate Nb-based cables. The dashed horizontal line represents the cooling capacity of a Bluefors XLD400 DR cooler loaded with 1,000 lines. The star is the projected performance of YBCO-on-Kapton cable

Previously, we have demonstrated the feasibility of the transfer of epitaxial thin films of high-temperature superconductor YBCO on Kapton tapes [6]. The YBC-based cables can operate up to 90 K in a magnetic field exceeding 100 Tesla at 4 K [7].

Manuscript received ; accepted . Date of publication; date of current version . This work was supported by U.S. DOE Office of Science award DE-SC0021707. *(Corresponding author: Vyacheslav Solovyov.)*

V. F. Solovyov is with Brookhaven Technology Group, 1000 Innovation Road, Stony Brook, NY 11794, (slowa@brookhaventech.com).

Hyunwoo Kim and Paul Farrell is with Brookhaven Technology Group, 1000 Innovation Road, Stony Brook, NY 11794

Color versions of one or more of the figures in this paper are available online at http://ieeexplore.ieee.org.

Digital Object Identifier

A line manufactured from YBCO-on-Kapton material would have thermal conductivity low enough to enable a compact quantum computing system with > 10,00 interconnects, as shown in Fig. 1. Here we report an important advance of the technology: the feasibility of two-sided devices with metalized via fences used to suppress parasitic resonance modes.

II. Experiment

We used standard 12 mm wide 2G tape supplied by Super-Power Inc [8]. In our previous work [6], we used a one-step direct transfer of YBCO layer to Kapton, followed by patterning the YBCO layer with a fiber laser [6]. The one-step process

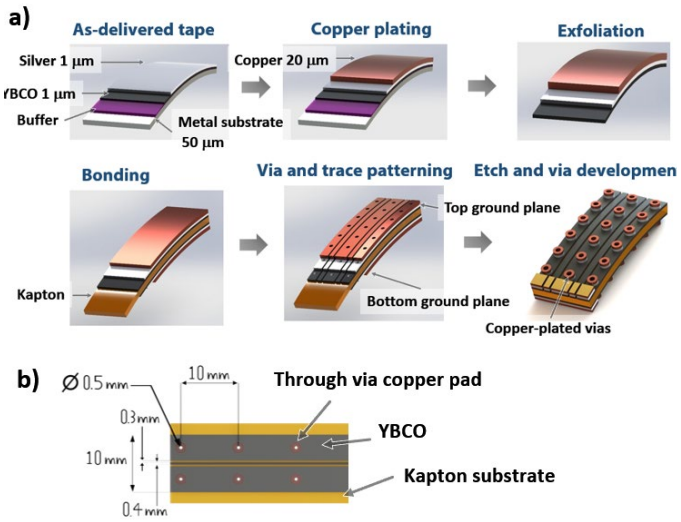

Fig. 2. a) Steps of manufacturing the two-side HTS coplanar with ground line by a two-step process. The Copper-Silver-YBCO laminate is first exfoliated from the substrate at the YBCO-buffer interface. Next, the laminate is bonded to a dielectric substrate, such as Kapton, FR4, or Duroid ®. b) Sketch of a coplanar with a ground line, showing the central signal line and row stitching vias.

demonstrated the feasibility of YBCO-on-Kapton technology. A serious limitation of this one-step approach is the unreliable metallization of the YBCO layer. Additionally, laser scribing proved poorly suitable for two-sided structures. After penetrating the top layer, the laser radiation damaged the bottom ground plane. Thus, the top and bottom layers had to be bonded after the patterning. Such an approach is thus difficult to implement for manufacturing multi-layer RF devices.

The improved two-step process utilized in this work is illustrated in Fig. 2a. The YBCO tape was plated with a 25 µm thick layer of copper by the manufacturer. The YBCO was exfoliated at the YBCO-buffer interface following the method previously described in [9]. After this step, the 1 µm thick YBCO film was supported by 25 µm thick copper foil, which allowed for easy handling. The foils were bonded YBCO-side to 127 µm (5 mil) thick polyimide (Kapton®, DuPont Corp.), FR4 or Duroid® (Rogers Corp.) substrates with Stycast 1266 epoxy. The resulting structure can be described as a two-sided FPCB. Importantly, in this arrangement, the YBCO-Copper contact was provided via a low-resistance and mechanically robust YBCO-silver interface, which greatly simplified bonding and via processing. The via hole (0.5 mm bore) pattern was drilled with a CNC machine (LPKF Protomat S100). Next, the boreholes

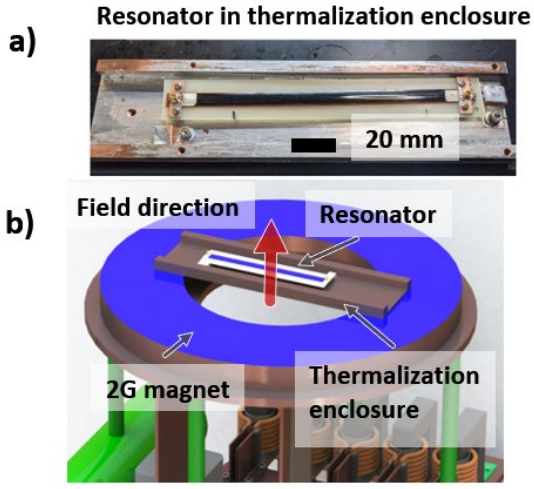

Fig. 3. a) 20 cm long coplanar resonator in a thermalization enclosure. b) Rendring of in-field test experiment: the thermalization enclosure and the resonator inside a conduction-cooled HTS magnet.

were coated with a thin conductive film, and finally, a 10 µm thick copper overlayer was deposited in an acid sulfate electroplating bath at 20 mA/cm^2 current density. The trace and via pattern were developed by the standard contact lithography using the dry-film photoresist (Riston FX2000, DuPont Corp.). In this work, we have chosen coplanar with ground (CPWG) RF line geometry. In order to determine the internal quality factor of the material, coplanar resonators were manufactured by laser-scribing coupling regions in the signal lines of a coplanar transmission line. Fig. 2b is a photograph of a typical 50 Ω CPWG line.

This type of line has been shown to enable high-density and low cross-talk. However, the low cross-talk between the lines can only be realized by a dense array of metalized vias that connect upper and bottom ground planes [10]. The initial via borehole coating proved to be the most challenging step of the process. In this work, we explored copper, nickel, and carbon ink methods. The electroless copper deposition followed the well-established sequence of $SnCl_2$ sensitization, $PdCl_2$ activation, and copper deposition from a basic copper solution. The Nickel metallization step started with the KOH hydrolysis step, followed by K-Ni ion exchange and reduction of Ni2+ ions to metallic Ni [11]. Finally, a thin film of Ni was deposited by an electroless process [12]. The carbon film was deposited by immersing the sample in an aqueous nano-carbon solution (Activator 310, LPKF Laser and Electronics Inc.).

Measurements up to 6 GHz were performed at 77 K using a Rohde & Schwarz ZNB series network analyzer. The setup for in-field measurement of the quality factor at 25 K is shown in Fig. 3. A YBCO resonator was placed in a thermalization enclosure manufactured from a 6 mm thick copper sheet. The resonator was placed inside a 2G magnet. A radiative thin film heater was placed immediately over the resonator in order to rapidly heat the resonator over the critical temperature.

III. Results and Discussion

Fig. 4b compares the critical current density, I_c, at 77 K of 10 mm wide, 1 μm thick YBCO films after transfer to Kapton (25 and 125 μm thick, see Fig. 4a) and 0.25 mm thick Duroid. After the transfer, the critical current density is retained within 20%

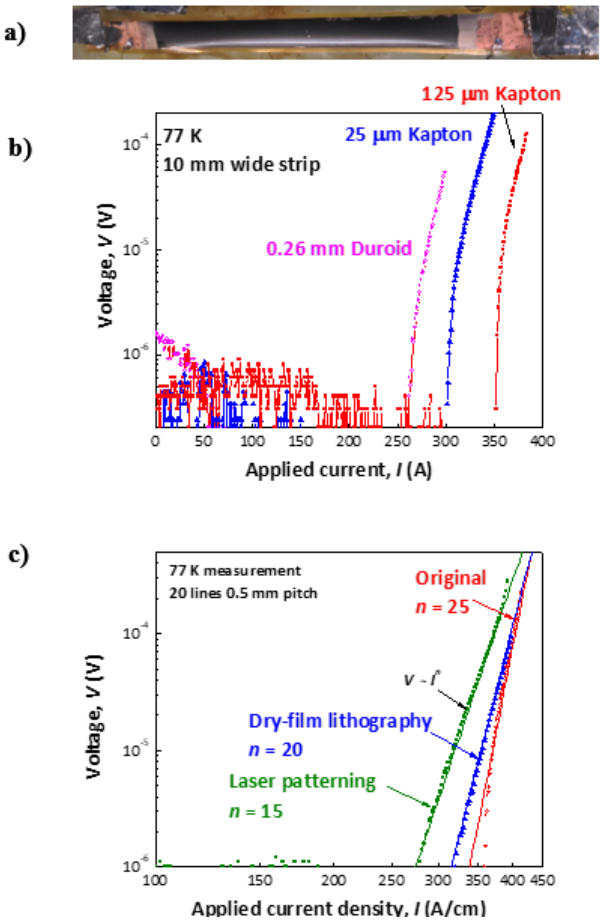

Fig. 4. a) A YBCO film on 25 μm Kapton film in a critical current measurement setup. b) Critical current density of 10 mm wide tape samples after transfer to Kapton (25 and 125 mm thick) and Rogers Duroid. c) Effect of patterning by laser and contact lithography Comparison of the critical current density of 77 K I-V curves of an original un-patterned 10 mm wide YBCO film on 0.125 mm thick Kapton tape. The solid lines are approximations of the data with the power law $V \sim I^n$.

of the original value 320 ± 30 A/cm. Fig. 4c shows the effect of patterning of the 10 mm wide tape in 10 0.5 mm wide spaced 1 mm apart. Here, we use the linear critical current density, A/cm, to account for the cross-section reduction after the patterning. The dry-film lithography is shown to be a less damaging process, as indicated by higher I_c and higher n-value of the lithographically processed sample, compared to the sample processed by laser scribing.

Fig. 5a is a series of resonant curves recorded during the cool-down of a crtitically coupled coplanar resonator in the cryogenic system shown in Fig. 3. The resonant frequency dependence on temperature is explained by the thermal contraction of the Kapton substrate. Fig. 5b is the time dependence of the resonant frequency after the sample is rapidly heated over the critical temperature. The solid curve is the prediction of a radiation-cooling model. The model takes into account the temperature dependence of the specific heat of Kapton and assumes the radiative heat transfer to the 25 K ambient. Here we use data in

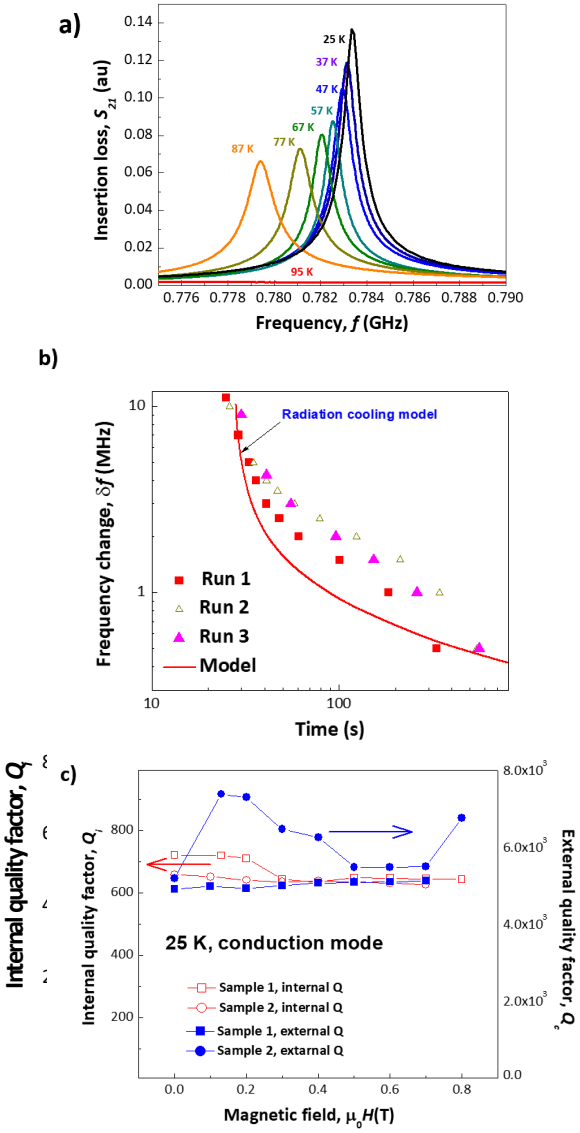

Fig. 5. a) The resonant curve of the first harmonic of the coplanar resonator at various temperatures. b) Frequency change of the resonator after heating over the critical temperature. The solid line is the prediction of the radiation cooling model. c) Magnetic field dependence of internal and external quality factors of critically coupled resonators at 25 K. The magnetic field was directed parallel to the c-axis (normal to the face of the resonator); see also Fig. 3.

Fig. 5a as a temperature-frequency calibration. The experiment proves that radiation cooling is the dominant heat transfer mechanism. This is expected considering the very low, 0.2 W/mK, the thermal conductivity of Kapton-YBCO at 25 K. Fig. 5c shows the dependence of internal and external quality factors of two critically coupled resonators. Here we use a numeric model proposed by Megrant *et al.* [13] to separate the external and internal quality factors. The magnetic field is observed to have a minor effect on the resonator quality. Recent measurements of the surface resistance [14] of commercial coated conductors from SuperPower, Fujikura, and Bruker, indicate that

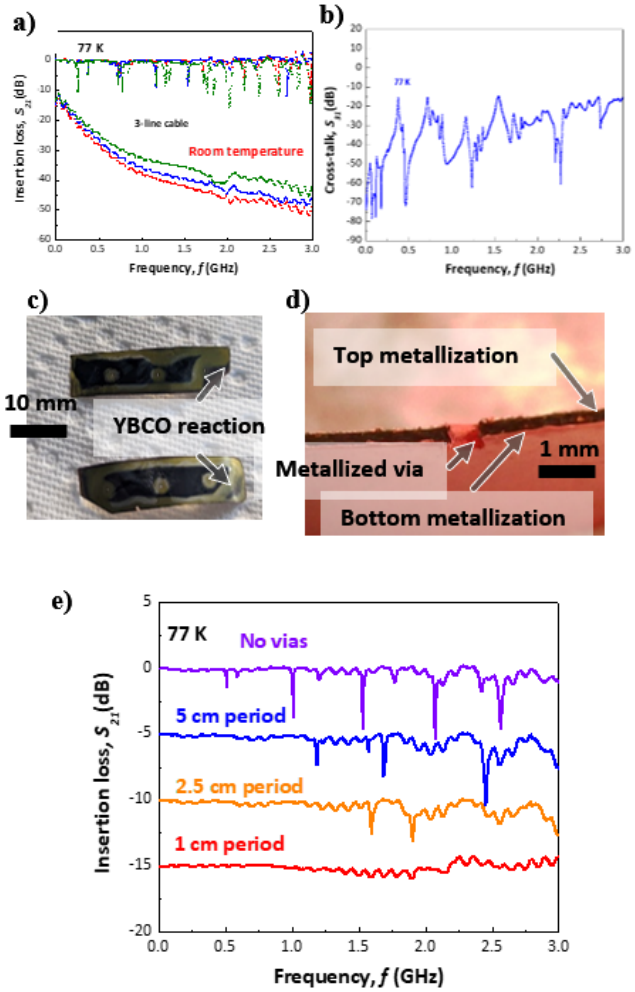

Fig. 6. a) The S_{21} spectra of individual lines in a three-line YBCO-on-Kapton cable at room temperature and 77 K. b) The S_{13} cross-talk spectrum, lines 1 and 2. c) Reaction of YBCO layer with the electroless copper bath. The white material around the vias and the tape edges is Y-Ba hydroxide forming after the reduction of Cu2+ ions to metal Cu. d) Cross-section of a metalized 0.5 mm via made by conductive carbon coating and copper electroplating. e) Frequency dependence of S_{21} parameter up to 3 GHz for 20 cm long CPWG lines without vias, with vias 5, 2.5, and 1 cm period. The S_{21} spectra show gradual suppression of parasitic resonance modes as the via period is shortened. The curves were numerically shifted by 5 dB for clarity.

surface resistance SuperPower YBCO at 8 GHz does not appreciably change up to 1 Tesla, 4 K from the zero field value of approximately 200 μΩ at 8 GHz. Numeric modeling of the resonator in Sonnet RF Suite suggests that at 25 K the quality factor of a YBCO resonator is dominated by dielectric loss, which is explained by the weak effect of the magnetic field on dielectric losses. Tests of a three-line 20 cm long CPWG cable without stitching vias, Fig. 6a, emphasize the importance of managing the parasitic resonances. At room temperature, all three lines exhibit high loss, consistent with high resistivity of YBCO in a non-superconducting state. At 77 the average loss < 1 dB at 3 GHz, however, multiple strong resonances are clearly visible. The parasitic resonant states can be described as standing waves between upper and bottom ground planes of a CPWG waveguide. The parasitic resonances contribute to high S_{13} cross-talk of the cable, – 30 dB, see Fig. 6b.

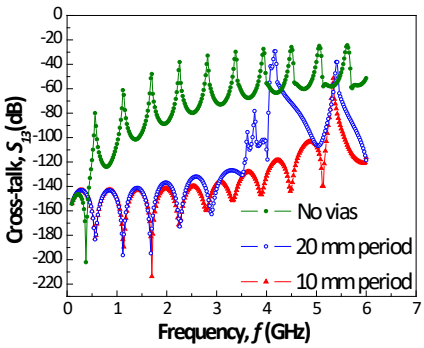

Fig. 7. Numeric modeling of S_{13} cross-talk in a 10 mm wide, two-line CPWG cable, without vias, and via fences with 20 and 10 mm period. A via fence with 10 mm period is predicted to deliver better than 60 dB inter-line isolation up to 6 GHz.

Attempts of electroless plating of vias by copper and nickel result in non-superconducting samples. Inspection of the YBCO layers reveals that the electroless plating solution aggressively reacts with the YBCO layer. The electroless plating relies on the catalytic reduction of Cu2+ ions in the solution to the metal Cu. The same reaction is apparently reducing Cu2+ ions in the YBCO structure to metallic copper and a mixture of Y and Ba hydroxides. The reaction products have a much lower density than YBCO, which leads to the delamination of the YBCO-Copper lamina from the Kapton substrate and the disintegration of the cable, Fig. 6c.

Coating the via bore with a conductive carbon proved the only method compatible with YBCO, that also delivered metalized vias reliably, as shown in Fig. 6d. Application of metalized via fence to a single line CPWG (see Fig. 2b) is shown in Fig. 6e. The S_{21} spectrum of a line without stitching vias contains several strong resonances. The introduction of vias with 5 and 2.5 cm period gradually suppresses resonances; a via fence with a 10 mm period delivers S_{21} curve that is resonance-free and flat within ± 1 dB.

The numerical model of the effect of the via fence period on the cross-talk, S_{13}, is presented in Fig. 7. Here, a cable with two 50 Ω, 0.4 mm wide lines separated by 3 mm wide ground planes stitched to the bottom ground plane with a via fence with a variable via density. The modeling result in Fig. 7b, is an encouraging confirmation that via fence isolation with 10 mm period will be effective in suppressing the cross-talk well below the benchmark, – 60 dB.

IV. Conclusion

In conclusion, we demonstrate the feasibility of manufacturing cryogenic devices based on two-sided YBCO-on-Kapton material using flexible PCB processing. The devices incorporate metalized vias, which are critical for suppressing parasitic ground plane resonances. The future effort will focus on reel-to-reel deposition of resist using thermoset jet-printable resist. The next crucial validation step is manufacturing a multi-line device with < – 60 dB isolation between the lines by a via fence.

REFERENCES

[1] J. P. Smith, B. A. Mazin, A. B. Walter, M. Daal, I. J. I. Bailey, C. Bockstiegel, N. Zobrist, N. Swimmer, S. Steiger, and N. Fruitwala, "Flexible Coaxial Ribbon Cable for High-Density Superconducting Microwave Device Arrays," *IEEE Trans. Appl. Supercond.,* vol. 31, no. 1, pp. 1-5, 2021, doi: 10.1109/TASC.2020.3008591.

[2] M. Daal, N. Zobrist, N. Kellaris, B. Sadoulet, and M. Robertson, "Properties of selected structural and flat flexible cabling materials for low temperature applications," (in English), *Cryogenics,* Article vol. 98, pp. 47-59, Mar 2019, doi: 10.1016/j.cryogenics.2018.10.019.

[3] A. B. Walter, C. Bockstiegel, B. A. Mazin, and M. Daal, "Laminated NbTi-on-Kapton Microstrip Cables for Flexible Sub-Kelvin RF Electronics," (in English), *IEEE Trans. Appl. Supercond.,* Article vol. 28, no. 1, p. 5, Jan 2018, Art no. 2500105, doi: 10.1109/tasc.2017.2773836.

[4] D. B. Tuckerman, M. C. Hamilton, D. J. Reilly, R. Bai, G. A. Hernandez, J. M. Hornibrook, J. A. Sellers, and C. D. Ellis, "Flexible superconducting Nb transmission lines on thin film polyimide for quantum computing applications," *Supercond. Sci. Technol.,* vol. 29, no. 8, p. 084007, 2016/07/11 2016, doi: 10.1088/0953-2048/29/8/084007.

[5] T. Braine, R. Cervantes, N. Crisosto, N. Du, S. Kimes, L. J. Rosenberg, G. Rybka, J. Yang, D. Bowring, A. S. Chou, R. Khatiwada, A. Sonnenschein, W. Wester, G. Carosi, N. Woollett, L. D. Duffy, R. Bradley, C. Boutan, M. Jones, B. H. LaRoque, N. S. Oblath, M. S. Taubman, J. Clarke, A. Dove, A. Eddins, S. R. O'Kelley, S. Nawaz, I. Siddiqi, N. Stevenson, A. Agrawal, A. V. Dixit, J. R. Gleason, S. Jois, P. Sikivie, J. A. Solomon, N. S. Sullivan, D. B. Tanner, E. Lentz, E. J. Daw, J. H. Buckley, P. M. Harrington, E. A. Henriksen, K. W. Murch, and A. Collaboration, "Extended Search for the Invisible Axion with the Axion Dark Matter Experiment," (in English), *Phys. Rev. Lett.,* Article vol. 124, no. 10, p. 6, Mar 2020, Art no. 101303, doi: 10.1103/PhysRevLett.124.101303.

[6] V. Solovyov, O. P. Saira, Z. Mendleson, and I. Drozdov, "YBCO-on-Kapton: Material for High-Density Quantum Computer Interconnects With Ultra-Low Thermal Loss," *IEEE Trans. Appl. Supercond.,* vol. 31, no. 5, pp. 1-5, 2021, doi: 10.1109/TASC.2021.3057010.

[7] G. Grissonnanche, O. Cyr-Choinière, F. Laliberté, S. René de Cotret, A. Juneau-Fecteau, S. Dufour-Beauséjour, M. È. Delage, D. LeBoeuf, J. Chang, B. J. Ramshaw, D. A. Bonn, W. N. Hardy, R. Liang, S. Adachi, N. E. Hussey, B. Vignolle, C. Proust, M. Sutherland, S. Krämer, J. H. Park, D. Graf, N. Doiron-Leyraud, and L. Taillefer, "Direct measurement of the upper critical field in cuprate superconductors," *Nature Communications,* vol. 5, no. 1, p. 3280, 2014/02/12 2014, doi: 10.1038/ncomms4280.

[8] Y. F. Zhang, T. F. Lehner, T. Fukushima, H. Sakamoto, and D. W. Hazelton, "Progress in Production and Performance of Second Generation (2G) HTS Wire for Practical Applications," (in English), *IEEE Trans. Appl. Supercond.,* Article vol. 24, no. 5, p. 7500405, Oct 2014, Art no. 7500405, doi: 10.1109/tasc.2014.2340458.

[9] V. Solovyov and P. Farrell, "Exfoliated YBCO filaments for second-generation superconducting cable," *Supercond. Sci. Technol.,* vol. 30, no. 1, p. 014006, 2017. [Online]. Available: http://stacks.iop.org/0953-2048/30/i=1/a=014006.

[10] G. E. Ponchak, E. M. Tentzeris, and J. Papapolymerou, "Coupling between microstrip lines embedded in polyimide layers for 3D-MMICs on Si," *IEE Proceedings - Microwaves, Antennas and Propagation,* vol. 150, no. 5, p. 344, 2003, doi: 10.1049/ip-map:20030545.

[11] T.-J. Liu, C.-H. Chen, P.-Y. Wu, C.-H. Lin, and C.-M. Chen, "Efficient and Adhesiveless Metallization of Flexible Polyimide by Functional Grafting of Carboxylic Acid Groups," *Langmuir,* vol. 35, no. 22, pp. 7212-7221, 2019/06/04 2019, doi: 10.1021/acs.langmuir.9b00354.

[12] M. P. M. Schlesinger, *Modern Electroplating*. John Wiley & Sons, 2011, p. 736.

[13] A. Megrant, C. Neill, R. Barends, B. Chiaro, Y. Chen, L. Feigl, J. Kelly, E. Lucero, M. Mariantoni, P. J. J. O'Malley, D. Sank, A. Vainsencher, J. Wenner, T. C. White, Y. Yin, J. Zhao, C. J. Palmstrøm, J. M. Martinis, and A. N. Cleland, "Planar superconducting resonators with internal quality factors above one million," *Appl. Phys. Lett.,* vol. 100, no. 11, p. 113510, 2012, doi: 10.1063/1.3693409.

[14] P. Krkotić, A. Romanov, N. Tagdulang, G. Telles, T. Puig, J. Gutierrez, X. Granados, S. Calatroni, F. Perez, M. Pont, and J. M. O'Callaghan, "Evaluation of the nonlinear surface resistance of REBCO coated conductors for their use in the FCC-hh beam screen," *Supercond. Sci. Technol.,* vol. 35, no. 2, p. 025015, 2022/01/07 2022, doi: 10.1088/1361-6668/ac4465.